

# Characterization of cornea-specific bioink: high transparency, improved in vivo safety

Journal of Tissue Engineering  
Volume 10: 1–12  
© The Author(s) 2019  
Article reuse guidelines:  
sagepub.com/journals-permissions  
DOI: 10.1177/2041731418823382  
journals.sagepub.com/home/tej



Hyeonji Kim<sup>1</sup>, Moon-Nyeo Park<sup>2</sup>, Jisoo Kim<sup>3</sup>, Jinah Jang<sup>3,4</sup>,  
Hong-Kyun Kim<sup>5</sup> and Dong-Woo Cho<sup>1</sup> 

## Abstract

Corneal transplantation is a typical surgical procedure for severe corneal diseases. However, the waiting time for a donor cornea has gradually increased due to a decrease in supply caused by an aging population and increased cases of laser-based surgeries. Artificial corneas were developed to meet the increase in demand; however, these approaches have suffered from material deterioration resulted by the limited tissue integration. Here, we introduce a cornea-derived decellularized extracellular matrix (Co-dECM) as a bioink for corneal regeneration. The developed Co-dECM bioink had similar quantitative measurement results for collagen and GAGs compared with that of the native cornea and also had the proper transparency for vision. The differentiation potential of human turbinate-derived mesenchymal stem cells (hTMSCs) to a keratocyte lineage was only observed in the Co-dECM group. Moreover, the developed bioink did not have any cytotoxic effect on encapsulated cells for three-dimensional (3D) culture and has great biocompatibility evident by the xeno-implantation of the Co-dECM gel into mice and rabbits for two and one month, respectively. An in vivo safety similar to clinical-grade collagen was seen with the Co-dECM, which helped to maintain the keratocyte-specific characteristics in vivo, compared with collagen. Taken together, the Co-dECM bioink has the potential to be used in various types of corneal diseases based on its corneal-specific ability and design flexibility through 3D cell printing technology.

## Keywords

Cornea, tissue engineering, decellularized extracellular matrix (dECM), bioink, biomaterials

Date received: 1 November 2018; accepted: 16 December 2018

## Introduction

The cornea, the transparent outermost tissue of the eye, has a pivotal role in eyesight because visible light is transmitted and refracted when passing through the cornea. Therefore, irreversible damage to the cornea can lead to loss of transparency, resulting in low vision or blindness in patients.<sup>1</sup> According to the World Health Organization, approximately 285 million people are suffering from visual impairments, mostly caused by corneal diseases. Although these patients can generally be treated by corneal transplantation, the average waiting time of 2134 days for a corneal transplant is the longest among all organ transplantations.<sup>2</sup> Moreover, the waiting time unfortunately has become even longer because of a shortage of donor cornea due to the rapid increase in the number of procedures for

- <sup>1</sup>Department of Mechanical Engineering and Center for Rapid Prototyping-based 3D Tissue/Organ Printing, Pohang University of Science and Technology, Pohang, Republic of Korea  
<sup>2</sup>College of Korean Medicines, Kyung Hee University, Seoul, Republic of Korea  
<sup>3</sup>School of Interdisciplinary Bioscience and Bioengineering, Pohang University of Science and Technology, Pohang, Republic of Korea  
<sup>4</sup>Department of Creative IT Engineering, Pohang University of Science and Technology, Pohang, Republic of Korea  
<sup>5</sup>Department of Ophthalmology, Kyungpook National University School of Medicine, Daegu, Republic of Korea

### Corresponding author:

Dong-Woo Cho, Department of Mechanical Engineering and Center for Rapid Prototyping-based 3D Tissue/Organ Printing, Pohang University of Science and Technology, 77 Cheongam-ro, Nam-gu, Pohang 37673, Gyeongbuk, Korea.  
Email: dwcho@postech.ac.kr



laser-based treatments and surgery (e.g., laser in-situ keratomileusis (LASIK)),<sup>3</sup> which makes the cornea undonatable. To replace donor corneas, clinically available synthetic corneas are widely being used including Keratoprosthesis (KPro, made of poly(methyl methacrylate) (PMMA)),<sup>4</sup> and AlphaCor™ (poly(2-hydroxyethyl methacrylate), PHEMA).<sup>5</sup> However, severe side effects from the artificial corneas have been reported after a long period because of foreign body reactions and the inappropriate properties of the materials, including different water contents and compositions from native tissues.<sup>6</sup> Based on these current limitations, many researchers have developed tissue-engineered corneas focusing on corneal characteristics such as transparency, biomimicry, and biocompatibility.

The most widely applied platform for corneal tissue engineering is a collagen hydrogel-based construct.<sup>7–12</sup> Merrett et al.<sup>7</sup> used type III collagen crosslinked with 1-ethyl-3-(3-dimethylaminopropyl)carbodiimide (EDC) and N-hydroxysuccinimide (NHS), which provided higher optical and mechanical properties compared with type I collagen, as the main corneal component. Four years after clinical transplantation, corneal re-epithelialization was observed; however, endogenous keratocytes and neural cells were hardly recruited into the center of the corneal graft.<sup>8</sup> Furthermore, these studies had some issues that the residual EDC and NHS produce cytotoxic products, and the central cell-free zone causes the material degeneration over a long period. Although these data were significant and translated in the clinic, the results revealed that cell-free systems invariably have a limitation in integrating the nearby stromal cells, leading to incomplete healing. To overcome this limitation, cell-laden collagen scaffolds were suggested.<sup>13–17</sup> Nam et al.<sup>13</sup> aligned corneal fibroblasts on a patterned 2- $\mu$ m thick collagen film fabricated by casting methods. The seeded cells secreted extracellular matrix forming sheet-type structures. After 2 weeks of culturing, the sheets were detached from the collagen films and manually stacked to build three-dimensional (3D) corneal constructs. However, it lost its transparency and was also easily separated from each sheet. To overcome this problem, Ghezzi and colleagues used transparent RGD surface-coupled patterned silk films.<sup>18</sup> They stacked 7 layers of cell-seeded silk film orthogonally and cultured the stacked constructs for 9 weeks. However, the obtained corneal equivalents showed a decrease in transparency when compared with a single film. Because stacking methods have limitations related to the transparency, some researchers have suggested direct fabrication of corneal equivalents using 3D cell printing technology.<sup>19</sup> Isaacson and colleagues have shown the feasibility of a 3D cell-printed cornea made of collagen and alginate with keratocytes. This proof-of-concept study confirmed the viability of the encapsulated cells but still requires more analysis on the corneal functions.

Recently, decellularized corneas have been suggested as a promising material for corneal equivalents with their tissue-specific properties and high biocompatibility. Hashimoto and colleagues prepared acellular corneas through physical treatments specifically using a high hydrostatic pressure.<sup>20</sup> Although the products had mechanical and optical properties similar to those of the native cornea, this system was not found suitable to be implanted because of its high rigidity, leading to an insufficient recruitment of stromal cells. Other research groups also used acellular corneas by chemical decellularization.<sup>21,22</sup> However, limited tissue integration was reported as well caused by the different properties between the implants and the native tissue. While decellularized corneas have many advantages, they have been revealed to have critical limitations in their use immediately after decellularization. Therefore, we suggest transforming the form of the decellularized cornea into a type of hydrogel to improve its tissue integrity and cell-recruitment capability.

Herein, we developed a cornea-derived decellularized extracellular matrix (Co-dECM) bioink, which can overcome the abovementioned limitations. The Co-dECM bioink, which is capable of 3D printing with encapsulated cells, is optically transparent, biochemically similar to the native cornea, and compatible *in vivo*. After preparing the Co-dECM bioink, the optical, physical, and biochemical characteristics were evaluated by transmitting light, observing the inner structures, and assessing gene expression using stem cells. The rheological properties of the bioink were also investigated, followed by performing the printing process and studying the viability of the printed cells. After the *in vitro* study, the *in vivo* biocompatibility and immunogenicity of the materials were also investigated.

## Materials and methods

### *Decellularization of cornea*

The whole corneas were prepared from bovine eyeballs, which were purchased from a slaughterhouse in GiGye, Korea. The corneas were washed using phosphate-buffered saline (PBS) solution containing penicillin (100 U/mL) and streptomycin (0.1 mg/mL). Then, we removed the epithelium and the endothelium from the cornea tissue to obtain pure stromal layers. These stromal tissues were stirred in 20 mM ammonium hydroxide solution (NH<sub>4</sub>OH; 4.98 N, Sigma-Aldrich, USA) containing 0.5% Triton X-100 (99.9% purity, Bio-Sesang, Korea) in distilled water. After 4 h, the tissues were immediately rinsed with distilled water and treated in the hypotonic tris hydrochloride (Tris-HCl, pH 7.4, Bio-Sesang, Korea) buffer solution for 24 h. Following stirring in 10 mM Tris-HCl containing 1% (v/v) Triton X-100 for 24 h at 37°C, the tissues were immersed in PBS solution for 48 h. The decellularized

tissues were sterilized with 1% peracetic acid (32 wt% in dilute acetic acid, Sigma-Aldrich, USA) solution in 50% ethanol for 10 h. After sterilization process and washing thrice times with PBS solution, the samples were rinsed with ultrapure water. When finished, the Co-dECM samples were lyophilized overnight. The prepared Co-dECM samples can be stored at  $-20^{\circ}\text{C}$  for 6 months.

### Characterization of Co-dECM

To validate the decellularization effects, the contents of DNA and the main components (collagen and glycosaminoglycans (GAG)) in native cornea and Co-dECM were quantified. Before conducting assays, the digested solutions of native cornea as control and Co-dECM should be prepared through incubating 10 mg of tissues in 1 mL of papain solution (125 mg/mL papain in 0.1 M sodium phosphate solution containing 5 mM  $\text{Na}_2$ -ethylenediaminetetraacetic acid (EDTA) and 5 mM cysteine-HCl at pH 6.5) for 16 h at  $60^{\circ}\text{C}$ . Papain solution without a tissue was also incubated as a blank and diluent buffer.

The double-stranded DNA content was determined using DNA purification kit (Thermo Scientific, USA) according to the manufacturer's instructions. The contents of sulfated GAG and total collagen were determined using 1,9-dimethylmethylene blue (DMMB) and hydroxyproline assay, respectively. For quantitative analysis of GAG, the absorbance at a wavelength of 530 nm was measured using a microplate reader by referring to a standard curve made from chondroitin sulfate A (Sigma-Aldrich, USA). Similarly, the collagen content was determined from a standard curve using hydroxyproline and the absorbance at 540 nm. All samples were assessed in triplicate.

### Co-dECM gel preparation and growth factors analyses

Lyophilized Co-dECM was crushed into powder using liquid nitrogen and a milling machine. An amount of 0.2 g of Co-dECM powder was digested in 10 mL solution of 0.5 M acetic acid (Merck, USA) containing 0.02 g pepsin (Sigma-Aldrich, USA) for Co-dECM powder for 3 days. After complete solubilization of Co-dECM, the solution was filtered through a filter with a pore size of 100  $\mu\text{m}$  and neutralized to pH 7.0–7.4 with 10 M sodium hydroxide NaOH (Sigma-Aldrich, USA) solution for cell culture. The pH-adjusted Co-dECM pre-gel was stored in a refrigerator at  $4^{\circ}\text{C}$ .

Afterwards, the Co-dECM gel samples were analyzed for determination of growth factor content with Col as a control using a Quantibody Human Growth Factor Array (RayBiotech, USA). Co-dECM gel and Col (1 mL aliquots) were prepared as described above for analysis.

### Rheological examinations

The rheological characteristics of 0.5% (5 mg/mL), 1.0% (10 mg/mL), 1.5% (15 mg/mL), and 2% (20 mg/mL) of Co-dECM gel samples were examined with Advanced Rheometric Expansion System (TA Instruments, USA). A steady shear sweep analysis of the Co-dECM gel was performed at  $15^{\circ}\text{C}$  to evaluate its viscosity. A dynamic frequency sweep analysis provided the frequency-dependent storage ( $G'$ ) and loss ( $G''$ ) moduli of Co-dECM gel.

### Light transmission examination

Corneal transparency was examined through measurement of the light transmittance using a microplate reader. Each 50  $\mu\text{L}$  sample of Col and Co-dECM gel was put into each well of a 48-well plate to become the same height as native cornea (about 500  $\mu\text{m}$ ) and gelled in the  $37^{\circ}\text{C}$  incubator. The Col solution was prepared through dissolving 0.2 g of collagen sheet (Dalimtissen, Korea) in 10 mL of 0.5 M acetic acid solution. As a control, native human cornea was prepared after dehydration through dipping in glycerol. The Institutional Review Board approval of the hospital ethics committee was obtained for use of human tissue (IRB No. KNUH 2013-11-016), and the Declaration of Helsinki was followed throughout this study. After setting the well plate in the microplate reader, the light absorption values in the wavelength range of 300–700 nm were determined. The light transmittance (T) values were calculated from the measured light absorbance (A) using the below equation

$$T(\%) = \frac{1}{10^A} \times 100$$

### Scanning electron microscopy

To observe internal structures, the experimental specimens of Co-dECM gel, Co-dECM gel mixed with Col in 5:5 ratio, and Col were prepared by crosslinking and examined with scanning electron microscopy (SEM) system. All specimens were cut into smaller than 1.5 mm specimens and rapidly cryofixed. Frozen specimens were immersed in 2.5% glutaraldehyde solution at room temperature for 12 h. Samples, after washing with PBS solution, were embedded in ethanol. After 2 h, samples were rapidly frozen in liquid nitrogen and then freeze-dried. They were coated with gold using a sputter-coater (Eiko IB, Kyoto, Japan) and examined with SEM at an acceleration voltage of 10 kV.

### Gene expression analysis

Gene expression analysis was conducted to validate the keratocyte-specificity with Co-dECM. Human turbinate-derived mesenchymal stem cells (hTMSCs) were prepared

**Table 1.** Primer sequences for KERA, ALDH, and GAPDH.

Gene		Sequence (5'–3')
KERA	Forward	GCCTCCAAGATTACCAGCCAA
	Reverse	ACGGAGGTAGCGAAGATGAGGT
ALDH	Forward	CGTCCTGATGCAAGCATGGAAGC
	Reverse	CTCCCAACAACCTCCTCTATGGCT
GAPDH	Forward	CCAGGTGGTCTCCTCTGACTTC
	Reverse	GTGGTCGTTGAGGGCAATG

as previously described in detail.<sup>23</sup> Briefly, hTMSCs were obtained from the Catholic University of Korea, St Mary's Hospital and cultured in normal Dulbecco's modified Eagle's medium (DMEM, Gibco, USA) containing 10% (v/v) fetal bovine serum (FBS, Gibco, USA) and 1% (v/v) penicillin/streptomycin (Sigma-Aldrich, USA) at 37°C in a humidified 5% CO<sub>2</sub> atmosphere. On passage 3, the normal medium was replaced with a differentiation medium containing 10 ng/mL KGF/EGF for 1 day to obtain predifferentiated hTMSCs.<sup>23</sup>

Each 75 µL of Col and Co-dECM gel encapsulating predifferentiated hTMSCs ( $1 \times 10^6$  cells/mL) were put in each well of 96 well plate (n=3 per group) and incubated for 30 min at 37°C. To each well, 100 µL of normal medium was added, followed by culturing samples for 14 days at 37°C in a humidified atmosphere containing 5% CO<sub>2</sub>. The culture medium was changed every 3 days.

On days 7 and 14, the mRNAs were extracted from each sample using Trizol (Invitrogen Life Technologies, USA) and quantified using Nanodrop with RNA purification kit (Thermo-Fisher Scientific, USA). A total of 1 µg of RNA was synthesized into cDNA using the Maxima First Strand cDNA synthesis system (Thermo-Fisher Scientific, USA). After preparing the samples using an SYBR Green PCR Master Mix assay (Applied Biosystems, USA), real-time PCR experiment was conducted using an ABI 7500 Real-time PCR system (Applied Biosystems, USA). Primers were designed based on the previous study.<sup>23</sup> After denaturation at 95°C for 10 min, the amplification reaction was conducted for 40 cycles of annealing at 95°C for 15 s and extension and detection at 60°C for 1 min. The following primers were used: KERA, ALDH, and Glyceraldehyde 3-phosphate dehydrogenase (GAPDH) (Table 1). The gene expression levels were normalized to GAPDH and analyzed using 2- $\Delta\Delta$ CT method. Each sample was assessed in triplicate.

### Printability examinations

Our in-house 3D cell printing system was operated to study the 3D cell printing process.<sup>24</sup> Co-dECM bioink encapsulating cells were printed with consideration of the printing parameters: piston speed (21, 23, 25, 27 rad/s), feed rate (25, 50, 75, 100, 125, 150, 175, 200 mm/min),

and nozzle diameter (19G, 21G, 23G, 25G). During the printing process, the temperature of printing head was set at 4°C and that of printing bed at 37°C. The printed structures were thermally crosslinked after 30 min of incubation at 37°C. The line widths of three printed samples in each condition were measured, and the printing process was replicated five times.

Cell viability after printing was evaluated after 1-day culture. Samples were stained using live/dead assay kit (Invitrogen Life Technologies, USA) following manufacturer's protocol. Live and dead cells were visualized using Zeiss LSM 510 Meta confocal microscope (Zeiss, Jena, Germany).

### In vivo examinations

To examine the biocompatibility of Co-dECM bioink, animal experiments were conducted using mice and rabbits. Mice were used to observe the immune responses, because corneal cells are too quiescent to observe any kind of stimuli.<sup>25</sup> Afterwards, specimens were implanted in the rabbit models to examine the immune reactions and cell activities as well. Animals were treated according to the ARVO Statement for the Use of Animals in Ophthalmic and Vision Research. The approved methods for animal experimentations are as follows. The methods using two kinds of animals are explained below and all the specimens were implanted in gel form.

### Mouse model

Balb/c mice (n=6) were anesthetized with ketamine (1 mg/kg, Syntec, Brazil) and rompun (0.2 mg/kg, Bayer, Belgium). The dorsal fur was removed through shaving and then the skin antisepsis was treated with ethanol (70%). The experimental samples (Co-dECM gel, Col), prepared in a 50-µL volume, were aseptically implanted into a subcutaneous pouch through a 1-cm long dorsal midline incision. The operated animals were monitored for any sign of infection at the operative site, discomfort, or distress after operation.

### Rabbit model

Adult New Zealand 6-week-old white rabbits (female, 2.5–3 kg) were used (n=12) for in vivo study. The approved methods for animal experimentations are as follows.

Animals were anesthetized by intravenous injection of 35 mg/kg sodium pentobarbital (Somnopentyl, Kyoritsu Seiyaku Corporation, Tokyo, Japan), and topical 0.4% oxybuprocaine hydrochloride (Benoxil, Santen Pharmaceutical Company, Osaka, Japan). The in vivo behavior of the experimental samples (Co-dECM gel, Col, Co-dECM gel encapsulated cells, Col encapsulated cells) were prepared. Here, we used porcine type 1 atelocollagen (Coltrix™, Ubiosis, Korea) as Col. Each hydrogel (Co-dECM and Col) was crosslinked for 30 min in a mold with a diameter

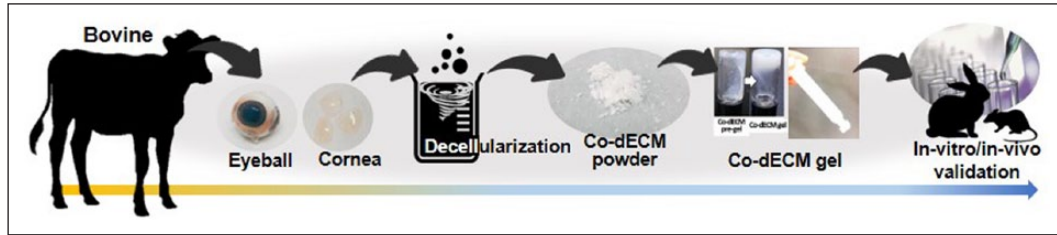


**Figure 1.** Schematic of Co-dECM gel preparation and its validation.

of 3 mm and a height of 100  $\mu\text{m}$ . For the cell-encapsulated samples, each hydrogel (Co-dECM and Col) was intermixed with cells and crosslinked in the same condition. Following that, the experimental samples (Co-dECM gel, Col, Co-dECM gel encapsulated cells, Col encapsulated cells) were transplanted to the rabbit corneal pocket model. Each group was prepared with three samples, and only one eye of each animal was used in the operations.

### Histological analyses

For each time interval, three implants from every group were fixed in 10% buffered formalin solution with pH 7.4 and processed for the paraffin embedding. Sections 5- $\mu\text{m}$  thick were stained with hematoxylin/eosin (HE) for histological and morphometrical analyses and May-Grunwald-Giemsa staining technique for inflammatory examinations.<sup>26</sup> Images of 25 fields per slide using a planapochromatic objective (20 $\times$ ) were obtained from light microscopy (Olympus BX-640) experiments. The images were digitalized through a JVC TK-1270/JGB microcamera and analyzed using an image analyzer software (Kontron Electronics, Carl Zeiss-KS300, version 2, Germany).

### Optical coherence tomography

The stability of implants and regenerated neo-corneas were assessed with examination of the changes in thickness and shape over time. Anterior segment optical coherence tomography system was used to monitor the changes in the corneal thickness. Two-way analysis of variance (ANOVA) analysis was used with a general linear model to compare the central corneal thickness with respect to the group and postoperative time. The nonparametric Mann-Whitney rank sum test was used where data did not satisfy equal variance testing for the comparison of central corneal thickness in operated groups versus normal healthy corneas. Statistics were performed using statistical software of SigmaStat (version 3.5 for Windows, Systat Software, Chicago, IL, USA).

### Immunofluorescence staining

The experimental samples were fixed with 4% (w/v) paraformaldehyde solution in PBS. The samples were

permeabilized with 0.1% Triton X-100 and were treated with 3% bovine serum albumin (Affimetrix, USA) in PBS solution for 1 h to block the nonspecific binding. The samples were washed with PBS solution thrice for 15 min. Anti-Human Keratocan antibody (LSBio, UK) were used as primary antibodies and treated overnight at 4°C. After washing with PBS solution, the samples were treated with Alexa Fluor 488 goat anti-mouse antibody (Invitrogen Life Technologies, USA) for 1 h at 37°C and counterstained with 4',6-diamidino-2-phenylindole (DAPI). Stained images were obtained with FV1000 Olympus confocal microscope (Olympus, Tokyo, Japan).

### Statistical analyses

All statistical data are expressed as a mean  $\pm$  standard deviation. Data were analyzed using two-way ANOVA followed by post hoc Tukey tests. For all comparisons,  $p < 0.05$  was considered statistically significant.

## Results

### Validation of remaining content in decellularized tissue

To develop a hydrogel mimicking the native cornea-like environment, corneal ECMs were acquired through decellularization and dissolved in an acidic solution. The efficacy was verified through in vitro and in vivo examinations (Figure 1).

Corneal ECMs, obtained by removing cells from the native corneas through chemical decellularization process, were validated by quantifying the amounts of remaining DNA, collagen, and GAG (Figure 2). The main purpose of decellularization process is retaining only ECMs without cells, which can cause an immune response, the most problematic of xenotransplantation.<sup>27</sup> To prevent immune rejection problems, decellularized tissue should have either less than 3% DNA relative to the native tissue, or no more than 50 ng/mg of double-stranded DNA content.<sup>28</sup> The prepared Co-dECM powder was found satisfying the standards; the residual amount of DNA was  $2.73\% \pm 0.009\%$  of the original cornea. However, the chemicals used in the decellularization process not only remove cells and residues but can also cause some damages to the extracellular

matrix. Thus, the efficacy of the decellularization process was quantified by measuring the amounts of collagen and GAG, typical components of corneal ECM, which were determined as  $76.50\% \pm 0.043\%$  and  $62.08\% \pm 0.034\%$ , respectively, relative to the original tissue. These results indicate that the prepared Co-dECM can provide complex cornea-specific biochemical cues similar to a native cornea while it reveals no serious immune response.

### Characterization of Co-dECM Gel

To verify the functional suitability of Co-dECM gel for corneal regeneration studies, we examined the physical

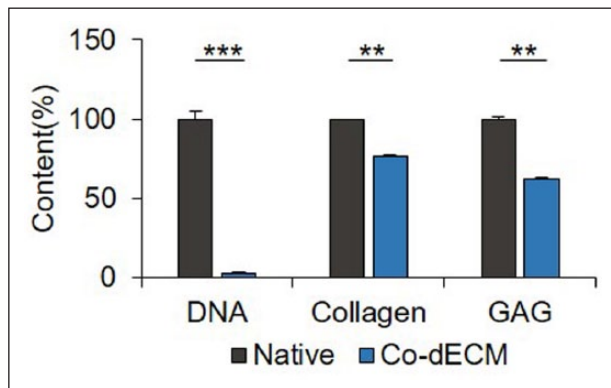


**Figure 2.** Quantification of remaining content in Co-dECM relative to the native cornea (\*\* $p < 0.01$ , \*\*\* $p < 0.005$ ).

(transparency and microstructure) and chemical (internal biomolecular growth factors) properties, and investigated gene expression pattern when stem cells are cultured on the gel. In this experiment, we chose two control groups: collagen hydrogel (Col, widely used for corneal regeneration study) and native human cornea. The 500- $\mu\text{m}$  thick (as the average thickness of native cornea<sup>29</sup>) Co-dECM gel showed higher transparency than that of the Col in visible light wavelength range of 390–700 nm (Figure 3 (a) and (b)).

According to the transparency criterion of artificial cornea, Co-dECM gel was evaluated as “Excellent” as the graft provides over 75% in the visible spectrum of light.<sup>30</sup> This superior optical transparency could be attributed to the thin collagen fibrils of the graft. Many studies have investigated that the optical transparency of the native cornea was originated from the thin collagen fibrils (~30–35  $\mu\text{m}$ ) and their close interfibrillar spacing, which are controlled by the interactions between collagen fibrils and proteoglycans located in the corneal stroma.<sup>31</sup> To investigate the transparency improvement by adding the native corneal ECM components such as proteoglycans, we measured the diameters of collagen fibers in Co-dECM gel (proteoglycan X1), Co-dECM gel mixed with Col in 5:5 ratio (proteoglycan X0.5), and Col (proteoglycan X0) using SEM images. The results showed that the larger amount of proteoglycan results in thinner collagen fibers associated with the higher transparency of Co-dECM gel (Figure 3 (c) and (d)). The thin collagen fibers might help to pass more

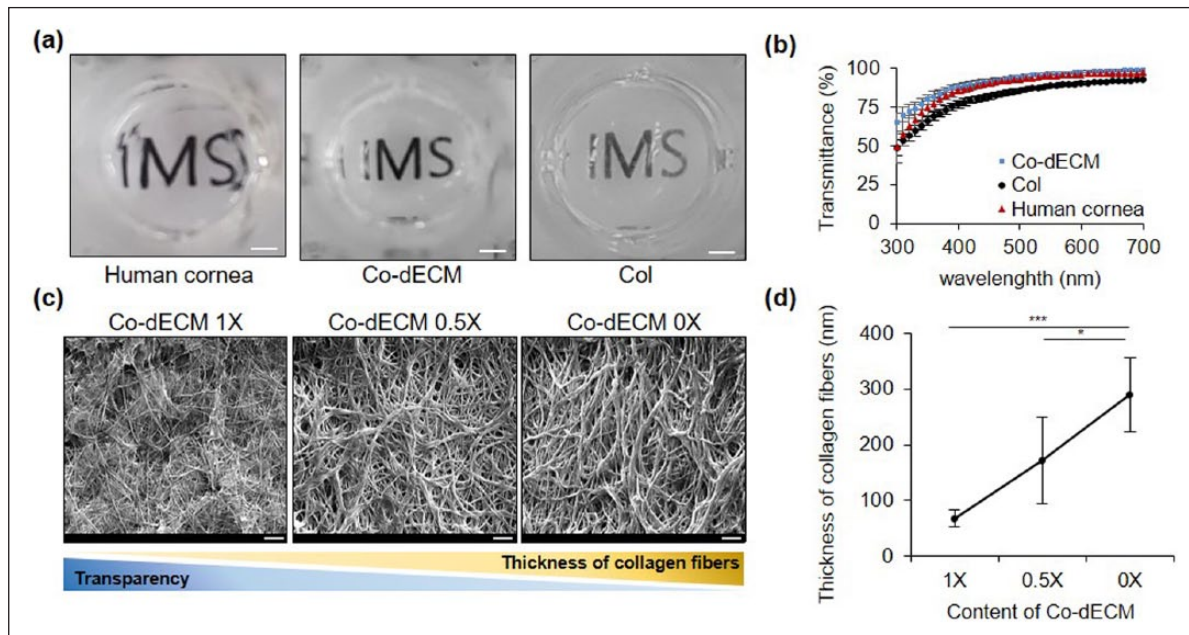


**Figure 3.** Optical properties of Co-dECM gel. (a) Gross images (scale bar: 2 mm). (b) Light transmittance variations of 2% Co-dECM gel, 2% Col, and human cornea at different wavelengths of visible light spectrum. (c) SEM micrographs of samples (scale bar: 10  $\mu\text{m}$ ). (d) Thicknesses of collagen fibers for Co-dECM gel (Co-dECM 1X), Co-dECM gel mixed with Col (Co-dECM 0.5X), and Col (Co-dECM 0X). \* $p < 0.05$ , \*\*\* $p < 0.005$ .

quantity of light through the graft, showing higher transparency for Co-dECM gel compared with Col only.

Furthermore, Co-dECM gel also contains various growth factors, including fibroblast growth factor (FGF), insulin-like growth factor (IGF), and transforming growth factor (TGF), which are abundantly observed in the native

**Table 2.** Growth factors and cytokine in native cornea, Co-dECM gel, and Col.

Growth factor	Amount (pg/mg)		
	Col	Co-dECM	Native cornea
AR	0	0	0
BDNF	0.8	0.5	0.5
bFGF	0	0	0
BMP-4	0	0	0
BMP-5	54.2	312.4	401.4
BMP-7	26.6	27.1	191.1
EGF	0.2	0.1	0.1
FGF-4	0	120.3	280.3
IGFBP-3	0	109.1	110.1
IGFBP-4	0	617.5	50.5
IGF-I	0	83.6	150.3
Insulin	15.3	58.5	59.7
MCSF R	0	11.8	0
NGF R	0	11	12.9
NT-3	0	27.6	11.8
NT-4	0	16.5	24.1
OPG	0	1.3	1.3
PDGF-AA	0	6.3	4.8
PIGF	0	6.7	10.8
SCF	0	5.6	9.9
SCF R	0	9.8	0
TGF $\alpha$	6.6	23.4	82.5
TGF $\beta$ 1	204.7	25.2	23
VEGF	0	0	1.4
VEGF R2	0	4.1	10
VEGF R3	0	6.8	2
VEGF-D	0	1.6	2.5
IL-10	0	5.8	4.6

cornea (Table 2).<sup>32</sup> In addition, we verified the biological effects of Co-dECM from the differentiation of stem cells into keratocyte lineage by culturing hTMSCs in the Co-dECM gel. The representative markers for cornea stromal layer, such as Keratocan (KERA), Aldehyde dehydrogenase (ALDH), were investigated after 14-day culture, expressed, respectively, as 7.30 and 11.97 times greater than the cells cultured in the Col gel (Figure 4). These results indicate that the Co-dECM bioink provides microstructural and biochemical cues for cells to induce them to differentiate into keratocyte lineage.

### Printability of Co-dECM bioink

To fabricate patient-specific artificial cornea, the developed materials should be printable as a bioink. We analyzed the rheological properties and then applied the Co-dECM bioink in printing process using the dispensing system. Co-dECM gel showed shear-thinning characteristics in shear stress range of 1–1000 s<sup>-1</sup>. Higher concentrated Co-dECM gel revealed larger viscosity values at shear rate of 1 s<sup>-1</sup>. Viscosity values at shear rates of 1 s<sup>-1</sup> for 0.5%, 1.0%, 1.5%, and 2.0% Co-dECM bioink samples were measured as 2.35, 3.83, 22.51, and 64.99 Pa s, respectively (Figure 5(a)). In addition, the Co-dECM gel samples showed a drastic decrease in the modulus change rate after a certain time at 37°C during experimentation, implying that Co-dECM gels were crosslinked. The time required for gelation of Co-dECM bioink with concentrations of 0.5%, 1.0%, 1.5%, and 2.0% were measured as 2201, 1151, 504, and 252 s, respectively. The modulus conversion at the time points occurred because the Co-dECM bioink contained collagen. That is, the collagen fibrils in the Co-dECM bioink samples with larger concentrations can be easily crosslinked, making the gelation times shorter. The 2.0% Co-dECM gel sample needed 8.7 times shorter gelation period than the 0.5% Co-dECM gel sample (Figure 5(b)).

Co-dECM gel was tested in printing process with controllable parameters, including various nozzle diameter,

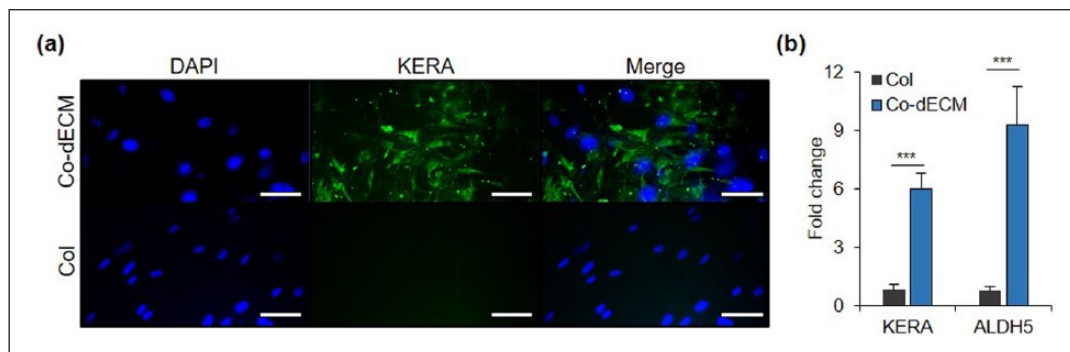


**Figure 4.** Gene expression analysis using predifferentiated hTMSCs encapsulated in Col and Co-dECM. (a) Immunofluorescence images stained with keratocyte-specific marker (KERA) and DAPI on day 14. (b) mRNA expression for cellular activity using Co-dECM and Col on days 7 and 14. (scale bar: 200  $\mu$ m, \*\*\* $p$  < 0.005).

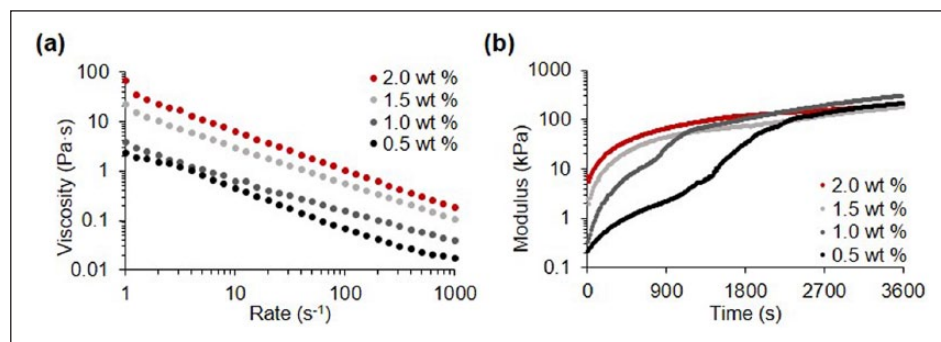


**Figure 5.** Rheological analyses of Co-dECM bioink. (a) Viscosity at 15 °C. (b) Gelation kinetics at 37 °C.

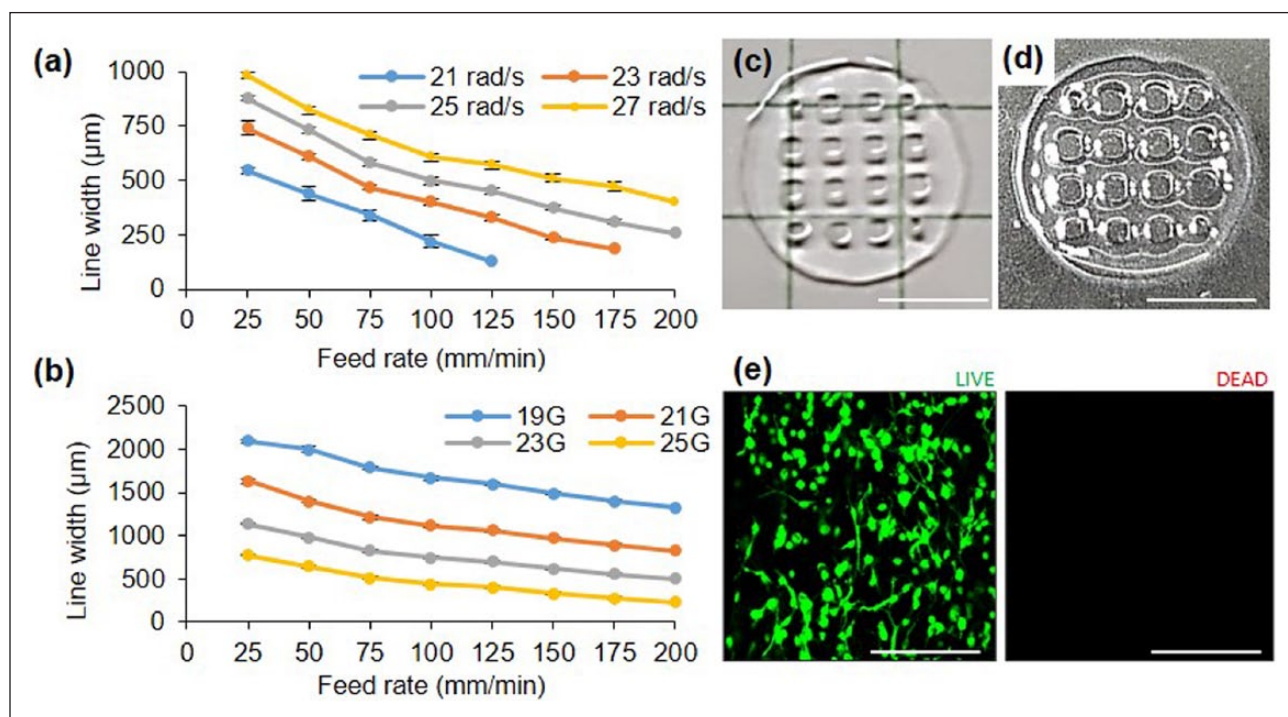


**Figure 6.** Printability evaluation depending on (a) piston speed and (b) nozzle size. Results of (c) 3D printing pattern (scale bar: 5 mm), (d) crosslinked construct (scale bar: 5 mm), and (e) cell viability examination of cell printed structure using 23G nozzle, speed 25, and 125 mm/min. (Green: live cells; Red: dead cells; scale bar: 200  $\mu\text{m}$ .)

piston speed, and head feed rate. The results indicate that the line width decreases as the printing or piston speed increases (Figure 6(a) and (b)). Furthermore, the needle diameter, which significantly affects the line width, was also observed as an important factor. When using 25 rad/s piston speed and a 25G nozzle with an inner diameter of 290  $\mu\text{m}$ , the line widths could be controlled in a range of 258–877  $\mu\text{m}$  (Figure 6(a)), while wide lines of 1327–2090  $\mu\text{m}$  could also be managed using a 19G nozzle at the same piston speed. Therefore, optimum nozzle size, printing speed, and pressure should be selected depending on the construct size and shape.

To assess the design flexibility of Co-dECM bioink, lattice pattern structures were printed (Figure 6(c)). The

printed structures maintained their printed pattern after crosslinking (Figure 6(d)). Moreover, no dead cells were observed in the Co-dECM structure, indicating that the cells were safely alive in Co-dECM bioink, even after printing process (Figure 6(e)). We would apply the obtained data to fabricate patient-customized cornea through 3D cell printing technology.

#### *Biocompatibility assessment*

After in vitro validation of Co-dECM bioink, the in vivo efficacy was evaluated. To observe the recruitment of immune cells, experimental specimens were implanted subcutaneously into mice prior to transplantation into the



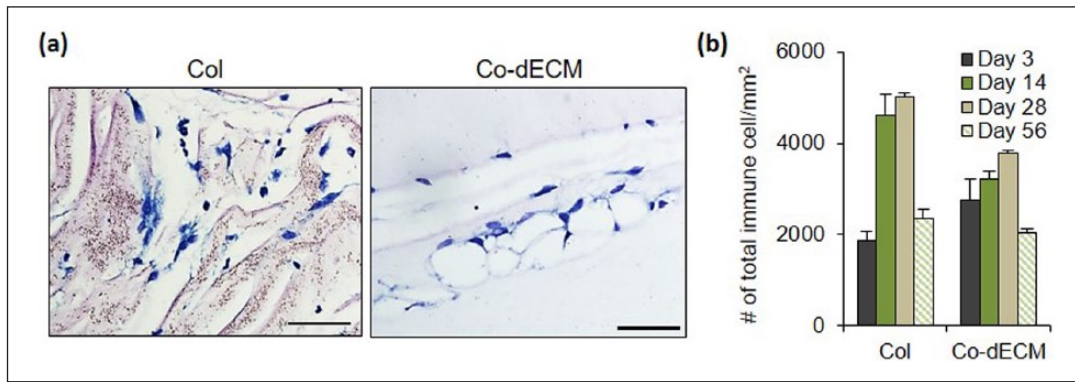


**Figure 7.** Inflammation test using mouse model. (a) Stained images on day 56 of implantation using May-Grunwald-Giemsa assay (scale bar: 200  $\mu$ m). (b) Number of stained cells on various days.

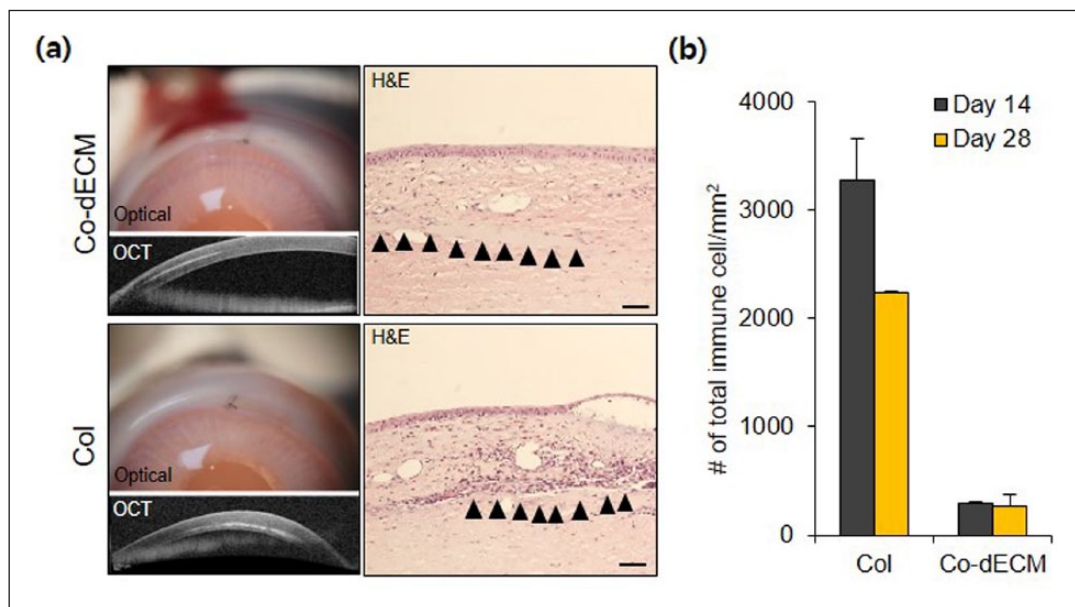


**Figure 8.** H&E stained images using rabbit model. Optical micrographs, OCT images with H&E stained images on day 28, and the number of immune cells on days 14 and 28. Scale bar: 50  $\mu$ m.

cornea, known as an immune-privileged tissue.<sup>17</sup> A Col group, which has been approved by Food and Drug Administration (FDA) as a clinical grade, was used as a positive control in the experiments. On the third day after transplantation of gels in the subcutaneous site of mice, the number of immune cells around Co-dECM gel was observed to be larger than that in Col, but the Co-dECM gel group revealed fewer immune cells without severe destruction after 2 months (Figure 7). Early days examinations after transplantation showed the immune cell recruitment as the acute host response, whereas the recruited immune cells disappeared over time. These results indicate that the implanted graft causes an innate foreign body reaction at the interface of the host tissue and the graft implantation.<sup>21</sup> After that, the same experimental groups were transplanted into the rabbit corneal pocket to observe

the immune response. The results showed fewer immune cells around Co-dECM gel than that in Col and tended to decrease along with transplantation days in all groups (Figure 8 and Supplementary Figure. 1). These results can be noted in the remained macromolecules in the Co-dECM, especially IL-10, which is known as the immunosuppressive protein, causing fewer immune responses compared with the medical-grade collagen (Table 1). Moreover, although we were concerned that corneal transplanted grafts can rapidly degrade in the *in vivo* environment,<sup>33</sup> the transplanted specimens maintained their original shapes (Figure 8), indicating the good immunocompatibility of Co-dECM gel similar to the clinic-grade Col.

*In vivo* tissue formation of hTMSCs encapsulated in Co-dECM gel was also examined with IF staining analysis using transplanted samples into cornea. Although there

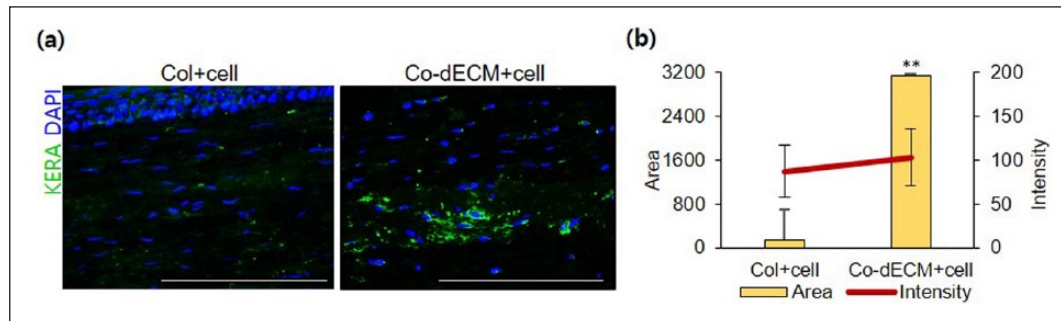


**Figure 9.** Immunochemical analyses after intrastromal pocket surgery using rabbit model. (a) Images of samples stained with KERA and DAPI on day 28. (b) Intensity and surface area values for KERA-stained cells (scale bar: 50  $\mu\text{m}$ ,  $**p < 0.01$ ).

were identical densities of cells, the area of KERA expression in Co-dECM gel group was found to be 21.13 times greater than that of Col gel group (Figure 9). These observations could indicate that the cells encapsulated in Co-dECM gel function better in vivo as keratocytes than the cells in Col.

## Discussion

This study demonstrated the ability to recapitulate the corneal specific microenvironment in the fabricated grafts using the bioink made from decellularized corneal tissues. This environment induced the differentiation of human turbinate mesenchymal stem cells into keratocyte-like cells expressing higher corneal specific markers (e.g., KERA). We also investigated the various characteristics of the Co-dECM bioink including the biological, biochemical, and biophysical properties in vitro and in vivo. In general, the aim of corneal tissue engineering is to fabricate optically, structurally, and biologically features similar to the native tissues.<sup>7–22</sup> However, the previously developed corneas had various difficulties achieving both optical and biochemical properties due to the origins of their applied biomaterials. Therefore, we suggested a Co-dECM hydrogel, not an opaque sponge or a sheet type of material, with a combination of cells to maximize the induction of the cornea recovery after the transplantation.

The purpose of the decellularization process is to avoid immune responses by removing all xenogeneic cellular components as well as immune rejection-related proteins. It has been reported that some macromolecules such as the telopeptides in the collagen and  $\alpha$ -gal protein in the cellular membrane usually induce antigenicity in humans; therefore, these should be removed during preparation or fabrication processes.<sup>27,34</sup> Particularly, many studies on the development of tissue-engineered corneas have used telocollagen, which can cause immune rejection and has not been approved for clinical use.<sup>13,19</sup> The use of the Co-dECM bioink can potentially exclude cellular remnants and such risky components including  $\alpha$ -gal protein by using a

chemical treatment. After the decellularization process, the Co-dECM was digested with the pepsin enzyme to degrade the telopeptides that are present at the end of the collagen polymers. It was shown through in vivo assessment that the Co-dECM gel causes little inflammation, which was similar to the level caused by medical-grade collagen. However, the residual pepsin should still be considered for clinical applications, and it can be dealt with using diafiltration, ion exchange, or salt precipitation methods.<sup>35</sup>

Furthermore, the Co-dECM gel has a high transparency due to the complex fibril structures.<sup>31</sup> The appropriate arrangement between the proper diameter of collagen fibrils and the fibril spacing enables visible light to be transmitted through the cornea which can be regulated by the proteoglycan content. The electrostatic forces from the charge of the proteoglycans and GAGs can control the balance in the collagen fibrils to maintain a transparent structure. In addition, the thin collagen fibrils in the Co-dECM group helped to reduce the light reflection, whereas the thick collagen fibrils in the collagen group scattered the light penetrating the samples. Therefore, the GAG content in the Co-dECM may have significant effects on regulating the assembly of the collagen fibrils, resulting in the Co-dECM bioink having a higher transparency than that of the pure collagen.

When the native cornea enables clear penetration of light, the corneal curvature focuses the image rays on the retina,<sup>1</sup> and eyesight is determined by the light refraction depending on the corneal curvature, thickness, and eye size. To fabricate a patient-specific artificial cornea, the curvature and thickness can be regulated and customized with 3D printing technology, which is a suitable technique to fabricate the desired shape of a structure with the cornea-specific Co-dECM bioink. We expect 3D printed corneas to have many beneficial effects such as high versatility, repeatability, and reproducibility for translational research. Taken together, further studies need to be conducted including on the arrangement of the collagen fibrils and the layered construction of cornea tissues before proceeding to clinical trials.

## Conclusion

We developed and verified the Co-dECM bioink that optically and biochemically provide cornea-mimicking micro-environment and can be adapted to the living body. The Co-dECM gel has cornea-specific properties and biocompatibility. We also showed that the versatility of the Co-dECM bioink was good to fabricate and maintain a 3D printed structure immediately after printing and after a 30-min crosslinking, during which all the cells remained alive as well. This study demonstrated the feasibility of Co-dECM bioink applications for the fabrication of patient-specific shaped artificial corneas. Thus, the proposed Co-dECM bioink can be applied to 3D cell printing technique to provide cornea-mimicking microenvironments. It may support progress in the field of cornea tissue engineering in future applications.

## Authors' note

Supporting Information is available from the Wiley Online Library or from the author.

## Declaration of conflicting interest

The author(s) declared no potential conflicts of interest with respect to the research, authorship, and/or publication of this article.

## Funding

The author(s) disclosed receipt of the following financial support for the research, authorship, and/or publication of this article: This work was supported by the Industrial Technology Innovation Program (Grant number 10048358), funded by the Ministry of Trade, Industry and Energy (MI, Korea); and by the MSIP (Ministry of Science, ICT and Future Planning), Korea, under the "ICT Consilience Creative Program" (IITP-R0346-16-1007) supervised by the IITP (Institute for Information & communications Technology Promotion).

## Supplemental material

Supplemental material for this article is available online.

## ORCID iD

Dong-Woo Cho  <https://orcid.org/0000-0001-5869-4330>

## References

- World Health Organization. *Universal eye health: a Global Action Plan 2014-2019*. World Health Organization, Geneva, [http://www.who.int/blindness/AP2014\\_19\\_English.pdf?ua=1](http://www.who.int/blindness/AP2014_19_English.pdf?ua=1) (2013, accessed 16 October 2018).
- Korean Network for Organ Sharing KONOS: annual report, [http://cdc.go.kr/CDC/cms/content/mobile/75/24275\\_view.html](http://cdc.go.kr/CDC/cms/content/mobile/75/24275_view.html) (2015, accessed 16 October 2018)
- Polisetti N, Vemuganti GK and Griffith M. Biomaterials-enabled regenerative medicine in corneal applications. In: Steinhoff G (ed) *Regenerative medicine-from protocol to patient*. Hamburg: Springer, 2016, pp. 97-122.
- Srikumaran D, Munoz B, Aldave AJ, et al. Long-term outcomes of Boston type 1 keratoprosthesis implantation: a retrospective multicenter cohort. *Ophthalmology* 2014; 121(11): 2159-2164.
- Crawford GJ. The development and results of an artificial cornea: AlphaCor™. In: Chirila T and Harkin D (eds) *Biomaterials and regenerative medicine in ophthalmology*, 2nd ed. San Diego, CA: Elsevier, 2016.
- Nouri M, Terada H, Alfonso EC, et al. Endophthalmitis after keratoprosthesis: incidence, bacterial causes, and risk factors. *Arch Ophthalmol* 2001; 119(4): 484-489.
- Merrett K, Fagerholm P, McLaughlin CR, et al. Tissue-engineered recombinant human collagen-based corneal substitutes for implantation: performance of type I versus type III collagen. *Invest Ophthalmol Vis Sci* 2008; 49(9): 3887-3894.
- Fagerholm P, Lagali NS, Ong JA, et al. Stable corneal regeneration four years after implantation of a cell-free recombinant human collagen scaffold. *Biomaterials* 2014; 35(8): 2420-2427.
- Zhang J, Sisley AM, Anderson AJ, et al. Characterization of a novel collagen scaffold for corneal tissue engineering. *Tissue Eng Part C Method* 2015; 28: 165-172.
- Riau AK, Mondal D, Aung TT, et al. Collagen-based artificial corneal scaffold with anti-infective capability for prevention of perioperative bacterial infections. *ACS Biomater Sci Eng* 2015; 1: 1324-1334.
- Parenteau-Bareil R, Gauvin R and Berthod F. Collagen-based biomaterials for tissue engineering applications. *Materials* 2010; 3: 1863-1887.
- Vrana NE, Builles N, Kocak H, et al. EDC/NHS cross-linked collagen foams as scaffolds for artificial corneal stroma. *J Biomater Sci Polym Ed* 2007; 18(12): 1527-1545.
- Nam E, Lee WC and Takeuchi S. Formation of highly aligned collagen nanofibers by continuous cyclic stretch of a collagen hydrogel sheet. *Macromol Biosci* 2016; 16(7): 995-1000.
- Wu J, Rnjak-Kovacina J, Du Y, et al. Corneal stromal bioequivalents secreted on patterned silk substrates. *Biomaterials* 2014; 35(12): 3744-3755.
- Wu J, Du Y, Mann MM, et al. Bioengineering organized, multilamellar human corneal stromal tissue by growth factor supplementation on highly aligned synthetic substrates. *Tissue Eng Part A* 2013; 19(17-18): 2063-2075.
- Crabb RA and Hubel A. Influence of matrix processing on the optical and biomechanical properties of a corneal stroma equivalent. *Tissue Eng Part A* 2008; 14(1): 173-182.
- Zhang C, Nie X, Hu D, et al. Survival and integration of tissue-engineered corneal stroma in a model of corneal ulcer. *Cell Tissue Res* 2007; 329(2): 249-257.
- Ghezzi CE, Marelli B, Omenetto FG, et al. 3D functional corneal stromal tissue equivalent based on corneal stromal stem cells and multi-layered silk film architecture. *PLoS ONE* 2017; 12(1): e0169504.
- Isaacson A, Swioklo S and Connon CJ. 3D bioprinting of a corneal stroma equivalent. *Exp Eye Res* 2018; 173: 188-193.
- Hashimoto Y, Hattori S, Sasaki S, et al. Ultrastructural analysis of the decellularized cornea after interlamellar keratoplasty and microkeratome-assisted anterior lamellar keratoplasty in a rabbit model. *Sci Rep* 2016; 6: 27734.

21. Du L and Wu X. Development and characterization of a full-thickness acellular porcine cornea matrix for tissue engineering. *Artif Organs* 2011; 35(7): 691–705.
22. PonceMarquez S, Martinez VS, McIntoshAmbrose W, et al. Decellularization of bovine corneas for tissue engineering applications. *Acta Biomater* 2009; 5(6): 1839–1847.
23. Park MN, Kim B, Kim H, et al. Human turbinate-derived mesenchymal stem cells differentiated into keratocyte progenitor cells. *J Clin Exp Ophthalmol* 2017; 8: 627.
24. Shim JH, Lee JS, Kim JY, et al. Bioprinting of a mechanically enhanced three-dimensional dual cell-laden construct for osteochondral tissue engineering using a multi-head tissue/organ building system. *J Micromech Microeng* 2012; 22: 085014.
25. Luo H, Lu Y, Wu T, et al. Construction of tissue-engineered cornea composed of amniotic epithelial cells and acellular porcine cornea for treating corneal alkali burn. *Biomaterials* 2013; 34(28): 6748–6759.
26. Lee KP, Kang S, Park SJ, et al. Anti-allergic effect of  $\alpha$ -cubebenoate isolated from *Schisandra chinensis* using in vivo and in vitro experiments. *J Ethnopharmacol* 2015; 173: 361–369.
27. Kim BS, Kim H, Gao G, et al. Decellularized extracellular matrix: a step towards the next generation source for bioink manufacturing. *Biofabrication* 2017; 9(3): 034104.
28. Garreta E, Oria R, Tarantino C, et al. Tissue engineering by decellularization and 3D bioprinting. *Mater Today* 2017; 20: 166–178.
29. Tai LY, Khaw KW, Ng CM, et al. Central corneal thickness measurements with different imaging devices and ultrasound pachymetry. *Cornea* 2013; 32(6): 766–771.
30. Ventura L, Jesus GT, Oliveira GC, et al. Portable light transmission measuring system for preserved corneas. *Biomed Eng Online* 2005; 4: 70.
31. Meek KM. Corneal collagen—its role in maintaining corneal shape and transparency. *Biophys Rev* 2009; 1(2): 83–93.
32. Kim A, Lakshman N, Karamichos D, et al. Growth factor regulation of corneal keratocyte differentiation and migration in compressed collagen matrices. *Invest Ophthalmol Vis Sci* 2010; 51(2): 864–875.
33. Huang YX and Li QH. An active artificial cornea with the function of inducing new corneal tissue generation in vivo—a new approach to corneal tissue engineering. *Biomed Mater* 2007; 2(3): S121.
34. Shim G, Kim MG, Park JY, et al. Small interfering RNAs (siRNAs) as cancer therapeutics. *Biomater Cancer Therap* 2013; 1: 237–269.
35. Jones RG and Landon J. Enhanced pepsin digestion: a novel process for purifying antibody F(ab')<sub>2</sub> fragments in high yield from serum. *J Immunol Methods* 2002; 263(1–2): 57–74.